

Study on the Fatigue Crack Growth of the 3D Surface of the Curved Steel Plate

Xinglu Wang*, Lile He

School of Mechanical and Electrical Engineering, Xi'an University of Architecture and Technology, Xi'an 710055, China
wangxinglu816@163.com

In the present study, the author researched on the fatigue crack growth of the 3D surface of the curved steel plate. The new conceptual design of the fatigue crack arrest device provides the user with flexible operating. The proposed device design consists of a handle, body, closed-circuit monitoring system assembly, nozzle, material flow nozzle, material tanks and piston assembly. The component can be repaired by laser; the laser flows to the nozzle central aperture. The curved steel plate channel outlets are around the nozzle aperture, material aligned at working focal point follow the laser beam. Presence and detection of a flaw by proximity sensor enable the repairing process. The temperature sensor enables the material flow once achieved the required set temperature. Piston assembly may follow the material flow process. These all processes are accomplished by a compact design. This novel conceptual design provides high degree of freedom to arrest the fatigue crack with simple mechanism. It demonstrates that the proposed technique alters the fatigue crack behaviour of the 3D surface of the curved steel plate with the proposed method.

1. Introduction

Fatigue fracture is known as one of the main failure modes in metal components of engineering structures. In order to prevent fatigue failure, numerous empirical law and theoretical analysis methods have been proposed to predict the fatigue life since the middle of the 19th century. Over the past few decades, continuing advances in modern machine, aerospace, ocean engineering have driven a substantial increase in the size of engineering structures as well as reduction in weight. Fatigue fracture of metal structures under high speed, high temperature and high loading conditions is a recurring challenge in modern industry. The investigations about the fatigue failure are always a great concern of scholars and engineers. The fatigue life of structures is predictable under give crack growth rates (Lin et al., 2015). Thus, most of the research attention about fatigue crack growth has been focused on the crack propagation speed before the crack reaches the critical failure length. The stress intensity factor ranges at a crack tip are proposed by Paris as governing parameters for fatigue crack growth rate in 1961. This landmark development established the theoretical basis for estimation of damage tolerance and fatigue life of engineering structures. However, series of experimental investigations in the past few decades have shown that the linear-elastic-fracture based Paris law is not capable of describing the fatigue crack propagating processes that dependents on the shape, size and the stress distributions of the plastic zone, such as the effects of load ratio, overload retardation, the transverse stress on biaxial fatigue as well as the propagation of physically short crack emanating from notch root.

People have recognized that the crack-tip plastic zone plays an important role in fatigue crack growth, and devote tremendous effort to introduce plastic zone as a mechanical parameter of fatigue failure criterion. However, the variation of the shape, size and stress distributions in the crack-tip plastic zone, which are loading history dependent, are extremely complex under variable cyclic loading conditions (Probst et al., 2015). The analytic models and mechanical parameters developed during past few decades are not sufficient to describe the property of crack-tip plastic zone. These models are not capable of interpreting the intrinsic relationship between fatigue crack growth behaviour and crack-tip plastic deformation. Therefore, how to describe the effect of the crack-tip plastic deformation on the fatigue crack growth behaviour is one of the most concerned projects that have not been fully addressed yet. Recently, our research group has developed an

approximate solution for the effect of crack-tip plastic deformation on stress intensity factor based on Esher by equivalent inclusion theory and transformation toughening theory. The solution provides rigorous and effective analysis methods to reveal the effects of the crack-tip plastic zone for fatigue crack growth behaviour in the metal materials (Lim et al., 2014).

For the study object in this paper, firstly, it should justify whether it belongs to fatigue problem, if so, fatigue life calculation method is in need. Then, fatigue strength correction is needed. It shows that the members in this paper suffer the fatigue accumulative damage. Thus, linear accumulative damage theory and nonlinear damage theory are used to calculate life separately. Then, making use of Finite Element method, fatigue life was also obtained. Comparing the three calculation results, it can be found that the results satisfy the requirement of the engineering design without the fatigue damage within the scope of the bearing load in project. But practical members broke up within a short use time. For this problem, using the reverse analysis and supposing the size of initial crack and applying the crack estimation formula that is most acceptable and the improved formula in the paper, the life was estimated for the crack member. In compared with actual cases, the results of the improved formula are more suitable for the crack propagation process. In the paper, the fatigue life was also being predicted with neural network intelligent technology. By this technology, the importance of each influencing factor on crack propagation was ranked. It shows that the initial angle, initial crack size and stress ratio are all the most important influencing factors. But that of the plate thickness is secondary. Moreover, the initial angle is more important than the initial crack size, which is very different from the past researches. It also shows that the importance of crack threshold is far more than that of fracture toughness, which isn't mentioned in the previous researches. All researches in the paper will be tested by more tests and data in future. And all works also present new aims of the fatigue researches.

2. Result and discussion

2.1 The model and algorithm

Fatigue is the phenomenon in which a crack develops and extends under cyclic stressing conditions, accounts for the vast majority of service failures. All types of materials are liable to fatigue fracture, but present-day knowledge is largely associated with crystalline solids, particularly metals and alloys. Consequently, the subject has been studied in depth by both engineers and metallurgists; the former being concerned with the endurance or lifetime of components under given fluctuating stresses, and the latter investigating the structural changes involve. Fatigue is progressive and localized structural damage that occurs when a material is subjected to cyclic loading and is one of the primary causes for catastrophic failure in structural materials. Enhancement of fatigue life is desired for improving utility of the materials.

The application of a stress, in surplus of the local yield value, to a crystalline material results in the production and movement of dislocations, which form slip bands or slip lines where they intersect the surface of the specimen. On repeated stressing the subsequent deformation is concentrated into certain of these slip steps, which become broader and deeper until eventually a micro-crack initiates. Incomplete reversibility of slip accounts for this process, but the precise dislocation mechanisms involved have not yet been unequivocally elucidated. Very thin folds of material known as extrusions are pushed out of the surface, and they are generally associated with small crevices, termed intrusions penetrating along the slip planes of maximum resolved shear stress. A stage I fatigue crack is simply an enlarged intrusion, and so any demarcation between initiation and stage I growth would appear unrealistic. The intrusion-extrusion mechanism may perhaps be regarded as the "classical" process of fatigue-crack initiation, although there are several other common sites at which cracks develop. These include interfaces of all types, and grain boundaries, particularly at high strain amplitudes and/or elevated temperatures. While intrusions and extrusions are being created at the surface, changes are also taking place within the interior of the specimen. A stable dislocation arrangement is set up, which is largely influenced by the cyclic stress amplitude and the stacking-fault energy of the material. A high value of the latter favours a continuous sub-grain structure, whereas in materials in which cross slip is difficult, islands of very high dislocation density occur in an essentially dislocation free matrix. It has been discussed at length these and other structural changes induced during fatigue-crack initiation. During this period also, significant alterations in mechanical properties may take place, which are of particular importance to the design engineer, who may employ the following empirical criterion to ascertain whether the strength has increased or diminished during cycling. As the intrusion or stage I crack extends along the active slip plane further into the body of the specimen, shear growth becomes more difficult due to the increasing tensile stress component. Eventually, the constraint is sufficient to cause a gradual macroscopic rotation of the crack to a non-crystallographic plane approximately normal to the direction of the applied stress, and this marks the onset of stage II propagation (Figure 1). The proportion of the total fatigue life spent in each stage is largely controlled by the stress amplitude. For small values of this, the majority of the life (up to 90) is taken up by the initiation and stage I growth processes, whereas at high cyclic stress levels stage II propagation may occupy a similar portion of the life. The existence of stress/strain concentrating features such as sharp comers, notches and large inter-metallic particles tends to inhibit or even eliminate the initiation and stage I aspects of fatigue-crack growth. This fact reinforces the earlier statement that in real

engineering components in which some stress concentrating feature can normally be found, stage II crack propagation is the most significant aspect of fatigue failure.

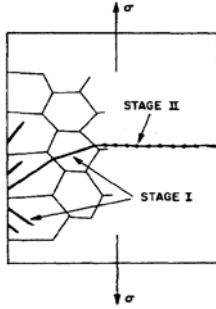


Figure 1: Schematic representation of the stages of fatigue- crack growth.

This aspect of crack growth has received by far the most attention both qualitatively and quantitatively; the impetus being generated largely as a result of the Comet disasters. The following section considered initially the qualitative information that has been provided by material scientists, and then examines the engineering attempts at measuring and predicting fatigue-crack growth rates. Avoided large stress concentrations, and a reasonable perimeters of security are taken to ensure that values close to the utmost admissible stress are never reached. However, material imperfections which originate at the time of production or usage of the material are ineluctable, and hence must be taken into account. Indeed even micro flaws may cause structures to fail, which are assumed to be safe, as they grow over time. The basic algorithm is shown as the following equation (1),

$$\text{Rule}(k) : \text{if } x_1 \text{ is } A_{1k} \text{ and } x_2 \text{ is } A_{2k} \cdots \text{and } x_n \text{ is } A_{nk} \quad (1)$$

$$\text{then } y = w_k, k \in \{1, 2, \dots, N\} \quad (2)$$

where x_i and y refer to the input variable and output variable, and the symbol A_{ik} refers to the precondition part. Furthermore, w_k means the output action strength that is corresponding to $\text{Rule}(k)$. Moreover, N refers to the number fuzzy rules, and n denotes the number of input variables. Based on the above definitions, the details of the fuzzy neural network model are explained as follows.

(1) Input nodes layer

In this layer, each node is regarded as an input variable, and the node only can transmit input values to its neighbour and upper layer.

$$v_i^1 = x_i, i \in \{1, 2, \dots, n\} \quad (3)$$

(2) Membership function nodes layer

In the second layer, nodes should be divided to N clusters, and then each cluster should follow a fuzzy rule. In particular, each node of this layer is able to calculate the value of membership function. Assume that an external input is represented as v_i^1 , and then the Gaussian membership function is described as followed.

$$v_{ij}^2 = \exp\left(-\frac{(v_i^1 - m_{ij})^2}{\delta_{ij}^2}\right), i \in \{1, 2, \dots, n\}, j \in \{1, 2, \dots, N\} \quad (4)$$

where m_{ij} and δ_{ij} refer to the centroid and the width of the Gaussian membership function respectively.

(3) Rules nodes layer

Different from the above layers, in this layer, the number of nodes means the number of fuzzy rules, and node in this layer is used to calculate the rule activation strength. Output values of this layer are listed in the following equation.

$$v_{ij}^3 = \prod_i v_{ij}^2, j \in \{1, 2, \dots, N\} \quad (5)$$

(4) Output nodes layer

Based on the above four layers, output values of this layer are computed as follows.

$$v^4 = \frac{\sum_j v_j^3 \cdot w_j}{\sum_j v_j^3} \quad (6)$$

The data obtained from the assessment sheet research development is the result of the development of table tennis learning media, the data validation results of three valuator, data from teacher and student

questionnaires, the data value of student learning outcomes. The data processing algorithm is shown in the following:

$$u_{c1} = \begin{cases} -(\omega_c t + \alpha_1 - 2\pi k) \frac{U_c'}{\pi} + U_c' & 2\pi k \leq \omega_c t < 2\pi k + \pi \\ (\omega_c t + \alpha_1 - 2\pi k - \pi) \frac{U_c'}{\pi} & 2\pi k + \pi \leq \omega_c t < 2\pi k + 2\pi \end{cases} \quad (7)$$

$$k = 0, \pm 1, \pm 2, \dots$$

The equation of sinusoidal modulation wave is:

$$u_s = U_s \sin \omega_s t \quad (8)$$

Set $F = \omega_s / \omega_c \gg 1$, modulation degree $M = U_s / U_c \leq 1$. For μ_{p1} , the sampling point is:

$$U_s \sin \omega_s t = -(\omega_c t + \alpha_1 - 2\pi k) \frac{U_c'}{\pi} + U_c'$$

Set $\omega_s t = Y$, $\omega_c t = X$, then $X = 2\pi k + \pi - \alpha_1 - \pi M \sin Y$

As shown in the form of $X = \omega_c t$ is in the interval between $2\pi k + \alpha$ and $2\pi(k+1) + \alpha$. Between 'a' and 'b', when the sine wave modulation is larger than the triangular carrier, the μ_{p1} is gotten. The time function of μ_{p1} is:

$$u_{p1}(X, Y) = \begin{cases} 0 & X \begin{cases} < 2\pi k + \pi - \alpha_1 - \pi M \sin Y \\ \geq 2\pi k + \pi - \alpha_1 + \pi M \sin Y \end{cases} \\ E/6 & X \begin{cases} < 2\pi k + \pi - \alpha_1 + \pi M \sin Y \\ \geq 2\pi k + \pi - \alpha_1 - \pi M \sin Y \end{cases} \end{cases} \quad (9)$$

The double Fourier series of function $\mu_{p1}(X, Y)$ is given:

In the above formula

$$A_{mn} + jB_{mn} = \frac{2}{(2\pi)^2} \int_{-\pi}^{\pi} \int_{-\pi}^{\pi} u_{p1}(X, Y) e^{j(mX + nY)} dXdY \quad (10)$$

Take the formula (9) into formula (10)

$$\begin{aligned} A_{mn} + jB_{mn} &= \frac{E}{j6mn} e^{jm(\pi - \alpha_1)} \left[J_n(mM\pi) \frac{e^{jn\pi} - 1}{2} - J_n(mM\pi) \frac{1 - e^{jn\pi}}{2} \right] \\ &= j \frac{E}{6mn} J_n(mM\pi) e^{jm(\pi - \alpha_1)} [1 - e^{jn\pi}] \end{aligned} \quad (11)$$

The we get:

$$\frac{\partial C}{\partial t} = D_L \frac{\partial^2 C}{\partial x^2} - u \frac{\partial C}{\partial x} \quad (12)$$

$$C(x, t)|_{t=0} = 0, \quad 0 \leq x < +\infty$$

$$C(x, t)|_{x=0} = C_0, \quad t > 0$$

$$C(x, t)|_{x \rightarrow +\infty} = 0, \quad t > 0 \quad (13)$$

2.2 The experiment result and discussion

So far, only the simplest cases of fatigue have been considered, i.e. fully reversed cycling with zero mean stress, and unidirectional cycling where the values of stress amplitude and maximum are identical. Crack propagation in real situations is more complex, and the influence on the basic equations discussed previously, of mean stress, cyclic frequency, and mode of testing will now be considered.

In most cases, fatigue involves stress fluctuations about a non-zero stationary stress, the magnitude of which would be expected to alter the extension rate of a growing crack. Generally, an increase in mean stress, C_m , leads to an increase in growth rate, but instances have been reported where there is no measurable effect. Relaxation at the crack tip has been put forward as a possible explanation for the latter. It is more usual to refer to the stress ratio, R (C_{Tmin} , G_{max}), and for a constant stress intensity range the cyclic crack growth rate increases as the value of R increases greater than zero. Changes in negative values of R have little effect on da/dN , indicating the minor influence of compression loading on propagation. The influence of test frequency arises from two sources; (a) environmental effects, and (b) strain-rate effects. Both are peculiar to the material under examination, although most information at hand fails to distinguish between them. At normal frequencies, the rate of crack propagation in metals increases as the cyclic frequency is reduced although in the ultrasonic range (~ 10000 Hz) there is some evidence that this tendency may be reversed. This may be due to a heating effect producing structural degradation as is the case in polymers at much lower

frequencies. Although this result cannot be directly equated with the propagation of a crack well removed from its initiation stage, it is reasonable that there should be a critical straining rate above which time dependent effects would become negligible. Information from square wave cycling tests, in which theoretically, the strain rate is infinite, should unequivocally reveal the influence of cyclic frequency. The stress wave-form (sinusoidal, square, saw tooth, etc.) may also influence crack growth to a secondary extent particularly at elevated temperatures, and not unexpectedly square wave cycling appears to be the most deleterious. The majority of service components are subjected not to uniaxial, but to multi-axial stresses/strains. It is therefore, pertinent to enquire, how useful is the wealth of data on uniaxial fatigue-crack propagation in assessing the durability of materials in real situations. The present paucity of information on cyclic crack extension under multi-axial conditions renders the question almost unanswerable, but the indications are that uniaxial data are of little quantitative assistance to the design engineer. Figure 2 shows the fatigue crack growth rate for the steel plate in different ageing conditions.

Figure 2. A comparison among the four ageing conditions of the alloy at various ΔK levels reveals that the crack growth rate of over-aged sample is much higher than that of T77 treated ones for the same ΔK . The crack growth rates of peak aged and under-aged samples are between those of the over-aged and T77 ones, and the under-aged sample exhibits a slightly lower fatigue crack growth rate than the peak-aged one. It indicates that the T77 temper offers the best fatigue crack growth resistance, the under-ageing comes next and the over-ageing shows the worst. Figs.3–6 show the microstructures of samples with under-ageing, peak-ageing, over-ageing and T77 temper, respectively. As for the under-aged sample, it is observed that very small precipitates uniformly distribute in the Al matrix, as shown in Figure 3(a). The average size is approximately 3 nm in length and 1 nm in width. The corresponding selected area diffraction pattern (SADP) in $[001]$ Al projection is shown in Figure 3(b). Apart from the diffraction spots of the Al matrix and Al_3Zr , another two sets of diffraction patterns could be observed. One is located at $\{1, (2n+1)/4, 0\}$, the other is located at $1/3$ and $2/3$ of $\{220\}$. According to the results of other According to the above statements, the degree of coherency of the precipitates with the Al matrix would be considered the first influence on the fatigue crack growth rate of the alloy. In the present work, due to the coherency of the main precipitates with the Al matrix lattice for under-ageing and T77 conditions (shown in Figs.3(c) and 6(c)), these precipitates are mainly sheared by the dislocations, promoting planar slip and enhancing the reversibility of dislocation motion. Therefore, the fatigue crack growth rates of under-aged and T77 treated samples are low. As for peak-ageing condition, in contrast, some η' precipitates that have a lower degree of coherency with Al matrix lattice form (Figure 4) and they would be non-sharable, resulting in a higher fatigue crack growth rate of peak-aged sample as compared with the under-aged and T77 treated ones, as shown in Figure 2.

The over-aged sample shows the highest crack growth rate because the main precipitate is η phase, which is incoherency with Al matrix lattice (Figure 5(c)) and not sharable in nature. Therefore, the reversibility of dislocation motion during the unloading is reduced by the η phases. On the other hand, the coarser and non-sharable η particles which form within the grain of the over-aged materials may promote void formation by continued plastic flow around them, which makes the fatigue crack propagate at a much higher rate. On the other hand, the precipitates in grain boundary and PFZ adjacent to the grain boundary may also influence the fatigue crack growth rate. It is known that the soft PFZ adjacent to the grain boundary offers less resistance to the deformation as compared to the grain interior. Therefore, it leads to easy formation of voids on coarse grain boundary particles and promotes the crack propagation.

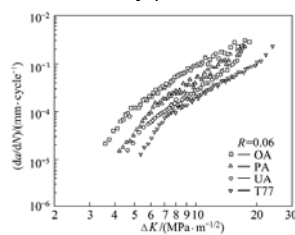


Figure 2: Fatigue crack growth rate for alloys in different ageing conditions

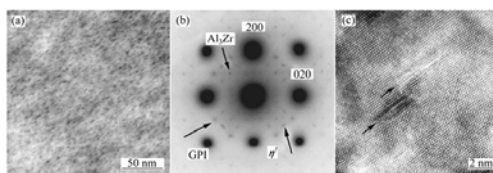


Figure 3: $[110]$ Al TEM image (a), $[001]$ Al SADP (b) and $[011]$ Al HRTEM image of η' phases (c) of inside grains of sample after under-ageing treatment

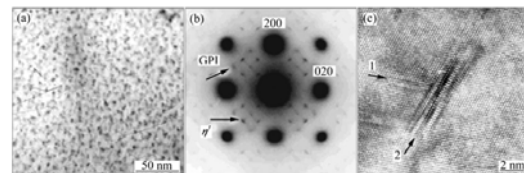


Figure 4: $[110]$ Al TEM image (a), $[001]$ Al SADP (b) and $[011]$ Al HRTEM image of η' phases (c) of inside grains of sample after peak ageing treatment

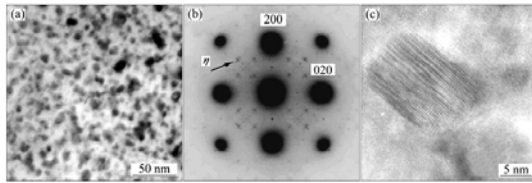


Figure 5: [110]Al TEM image (a), [001]Al SADP (b) and [011]Al HRTEM image of η phase (c) of inside grains of sample after over-ageing treatment

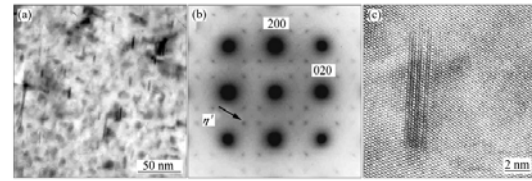


Figure 6: [110]Al TEM image (a), [001]Al SADP (b) and [011]Al HRTEM image of η' phase (c) of inside grains of sample after T77 treatment

In the present work, compared to the under-aged sample, the T77 treated sample is characterized by a pronounced PFZ adjacent to the grain boundary and coarse precipitates in grain boundary (Figs. 7(a) and (c)). The crack growth rate of the T77 treated sample is higher than that of the under-aged one. However, it is found that the crack growth rate of the under-aged sample is higher than that of the T77 treated one. It indicates that the effects of grain boundary precipitates and PFZ on the fatigue crack growth resistance are less significant than that of precipitates within grain in the alloy. Although the features of the grain boundary for both over-aged and T77 treated samples are comparable, the fatigue crack growth rate of the T77 treated sample is much lower than that of the over-aged sample, which would attribute to the nature of the precipitates inside grains.

3. Conclusion

The modified constitutive relation for fatigue crack growth of metals proposed by this paper is further generalized in the following three aspects:

- (1) To introduce an unstable fracture condition into the crack growth rate curve in order to cover the whole Fatigue crack propagation regime;
- (2) To define a "virtual strength" to replace the yield stress in order for the constitutive relation to be applicable from "crack-fret" plain specifying to crack from fatigue limit to ultimate strength;
- (3) To introduce: an overload/under load parameter 3 for modelling the overload retaliation and under load acceleration.

The performances of this general constitutive relation are extensively studied in this paper and the following conclusions can be drawn:

- (1) A sigmoidal shape of the constitutive relation will imply a sigmoidal shape of S-N curves;
- (2) The general crack growth rate is able to explain many special behaviours of metal fatigue such as fatigue crack growth under stress effect and load sequence effect;
- (3) The fatigue life will be very sensitive to tire initial crack size of microstructural level and without explicitly considering this Factor, a large scatter will occur in the tested lives even for plain specimens.

Reference

- Lin Y.K., Yang J.N., 2015, A stochastic theory of fatigue crack propagation. *Aiaa Journal*, 23(23), 117-124.
- Probst E.P., Hillberry B.M., 2015, Fatigue Crack Delay and Arrest Due to Single Peak Tensile Overloads. *Aiaa Journal*, 12(3), 330-335.
- Lim H.J., Sohn H., Desimio M.P., 2014, Reference-free fatigue crack detection using nonlinear ultrasonic modulation under various temperature and loading conditions. *Mechanical Systems & Signal Processing*, 45(2), 468-478.
- Sohn H, Lim H.J., Desimio M.P., 2014, Nonlinear ultrasonic wave modulation for online fatigue crack detection. *Journal of Sound & Vibration*, 333(5), 1473–1484.
- Riemer A., Leuders S., Thöne M., 2014, On the fatigue crack growth behavior in 316L stainless steel manufactured by selective laser melting. *Engineering Fracture Mechanics*, 120(4), 15-25.
- Shamsaei N., Fatemi A., 2014, Small fatigue crack growth under multiaxial stresses. *International Journal of Fatigue*, 58(1), 126-135.